MDPI

Article

Comparison of the Application of High-Resolution Inductively Coupled Plasma Mass Spectrometry (HR-ICP-MS) and Collision/Reaction Cell Technology of Inductively Coupled Plasma Mass Spectrometry (ICP-CCT-MS) in the Determination of Selenium in Coal-Bearing Strata

Shumao Zhao [1,2,*]**, Rongkun Jia** [1,2]**, Qiuchan Han** [1,2]**, Niande Shang** [1,2]**, Kaiyan Teng** [1,2] **and Jiawei Feng** [1,2]

1   Key Laboratory of Coalbed Methane Resources and Reservoir Formation Process, Ministry of Education, China University of Mining and Technology, Xuzhou 221008, China

2   School of Resources and Geosciences, China University of Mining and Technology, Xuzhou 221116, China

*   Correspondence: zhaoshumao@cumt.edu.cn

Abstract: Selenium, a trace element of significant importance for human health and the environment, can be introduced into the environment through coal combustion. Accurate determination of selenium in coal and coal-bearing strata is essential for implementing effective management strategies and control measures to minimize potential risks to human health and the environment. This study introduces an improved approach for the determination of ^{77}Se in the medium resolution mode using HR-ICP-MS, effectively separating interference from doubly charged ions and enabling precise determination of selenium in coal-bearing strata. The relative errors of the standard reference samples obtained by HR-ICP-MS are between 0.65% and 6.33%, comparing to that of ICP-CCT-MS (1.58%–17.27%), prove the reliability of this method. Additionally, the X (bar)—S control charts obtained from HR-ICP-MS compared to ICP-CCT-MS demonstrate the superior stability of HR-ICP-MS in continuous determination. Consequently, though ICP-CCT-MS has better instrumental stability reflected through the internal standard recovery (ICP-CCT-MS:104.81%; HR-ICP-MS:80.54%), HR-ICP-MS is recommended as the preferred method for selenium determination in coal-bearing strata because of its high accuracy and good stability.

Keywords: selenium; HR-ICP-MS; ICP-CCT-MS; coal-bearing strata

1. Introduction

Coal, one of the most important global energy sources, has garnered significant attention in recent years due to the trace element it contains, which has implications for the environment and human health [1–7]. Among these elements, selenium (Se) plays a vital role in physiological functions for humans and animals when consumed in moderate amounts [8–12]. However, excessive intake of Se can lead to selenosis [13–16]. Additionally, selenium is environmentally sensitive, and excessive selenium may contaminate water bodies and inhibit plant growth [17–19]. During coal combustion, Se can be released into the atmosphere, posing risks to the environment and human beings [20–33]. Therefore, accurate determination of selenium in coal and coal-bearing strata holds great significance for the coal mining industry, environmental protection, and human health.

Various methods have been developed for determining selenium in coal-bearing strata. Traditional methods include atomic absorption spectrometry (AAS), atomic fluorescence spectrometry (AFS), and inductively coupled plasma atomic emission spectrometry (ICP-AES) [34–42]. While these methods provide a certain degree of accuracy and reliability, they present disadvantages such as complicated sample pre-treatment procedures that

result in prolonged and intricate analytical processes, as well as limited sensitivity for detection [37,38,40,42]. However, advancements in science and technology have introduced new determination methods to enhance accuracy and sensitivity. For instance, high performance liquid chromatography-inductively coupled plasma mass spectrometry (HPLC-ICP-MS) enables analysis and quantification of selenium morphology in coal [43–46], providing valuable insights into selenium's environmental behavior and biological effects. Furthermore, other analytical methods, such as collision/reaction cell technology of inductively coupled plasma mass spectrometry (ICP-CCT-MS) [47–51] and hydride generation atomic fluorescence spectroscopy (HG-AFS) [52–54], have also been applied in the determination of selenium in coal-bearing strata.

High-resolution inductively coupled plasma mass spectrometry (HR-ICP-MS), an improved method of ICP-MS, has gained widespread usage in trace element determination in coal-bearing strata [55–58]. However, limited discussions exist regarding interferences in the testing process of Se and its application in coal-bearing strata [24,51,59,60]. In this study, we conduct a systematic analysis of the suffered interferences of six natural isotopes of Se during mass spectrometry, propose a method for determining ^{77}Se at medium resolution, and evaluate the reliability of this method using standard reference samples. The method is also compared with ICP-CCT-MS to discuss their application for Se determination in coal-bearing strata in terms of accuracy, precision, and stability.

2. Methods and Materials

2.1. Instruments

The instruments used for the comparison of Se determination in coal-bearing strata were an Attom ES HR-ICP-MS (Nu Instruments, Wrexham, UK), equipped with a Teflon sampling system and a quartz torch with a quartz injector tube, and a ThermoFisher ICP-MS (X Series II, Waltham, MA, USA), equipped with an Automated 3rd Generation Collision Cell Technology (CCTED). An UltraClave microwave high-pressure reactor (Milestone, Sorisole, Italy) was used for sample digestion before testing under a load pressure of 50 bar. Ultrapure water (18.2 MΩ·cm), produced by Milli-Q IQ 7010 Ultrapure water system (Millipore, Guyancourt, France), was used in all experiments. A DuoPUR acid purification system (Milestone, Sorisole, Italy) was utilized for further purification of the HNO_3 (GR, 65%, v:v). All vessels used in the experiments were cleaned by the TraceCLEAN Automatic Acid Reflux System (Milestone, Sorisole, Italy) at 250 °C for 2.5 h.

2.2. Reagents and Gasses

A series of Se standard solutions consisting of 6 concentration levels (0, 1, 10, 30, 50, and 100 µg/L) were configured from the 100 µg/mL standard reference solution (Inorganic Ventures, CCS4). In order to check the stability of the instrument during testing, the internal standard stock solution was diluted from the 1000 µg/mL Rh reference solution (GSB 04-1746-2004, National Center of Analysis and Testing for Nonferrous Metals and Electronic Materials) to 10 µg/L.

The further purified guaranteed reagent HNO_3 (65%, v:v) and the metal–oxide–semiconductor (MOS) reagent HF (40%, v:v) were used for sample digestion. For the cooling, auxiliary, and nebulizer gas, ultrapure argon was used in both HR-ICP-MS and ICP-CCT-MS. In addition, the ultrapure (99.999% pure) mixed gas composed of 93.33% He and 6.67% H_2 was introduced as the collision gas in ICP-CCT-MS.

2.3. Investigated Samples

A total of five standard reference materials were chosen to be detected in order to evaluate the accuracy, including two bituminous coal samples (SRM 1632e and SRM 2685c) and two fly ash samples (SRM 1633c and SRM 2691) from the National Institute of Standards and Technology (NIST) and a rock sample (GSR-20) from the National Institute of Metrology, China (NIM). Moreover, a study area with coal-bearing strata from Qisheng

mine, Xingtai coal field, was selected to make a comparison between the two methods. A thorough description of all the investigated samples is listed in Table 1.

Table 1. Overview of the investigated samples.

Sample ID	Lithology	Description
SRM 1632e SRM 2685c	Bituminous coal	NIST Standard reference material
SRM 1633c SRM 2691	Coal fly ash	
GSR-20	Carbonaceous-siliceous shale	NIM standard reference material
QS-9-1 QS-9-2 QS-9-3 QS-9-4 QS-9-5	Bituminous coal	No.9 Coal Seam from Qisheng Mine, Xingtai Coal field, China (this study)
QS-9-R	Roof, silty sandstone	Qisheng Mine, Xingtai Coal field, China (this study)
QS-9-6M QS-9-7M QS-9-8M	Carbonaceous mudstone	
QS-9-F	Floor, mudstone	

2.4. Sample Digestion

Five milliliters of purified HNO_3 and two milliliters of HF (metal–oxide–semiconductor, MOS) were added to 50 mg of coal samples that were broken to less than 200 mesh, and five milliliters of HF (MOS) and two milliliters of purified HNO_3 were added to the non-coal samples, respectively. The samples were then put into the UltraClave reactor for digestion. The microwave digestion program is provided in Table 2. After the digestion, the samples were transferred to the 100 mL volumetric flask and diluted to 100 mL for further analysis. Details of the sample digestion were described by Li et al. (2014) [43].

Table 2. Microwave program for sample digestion. Modified from Li et al. (2014) [43].

Step	Time (min)	Temp (°C)	Pressure (bar)	Microwave Power (W)
1	8	60	100	1500
2	12	125	100	1500
3	15	160	130	1500
4	15	240	160	1500
5	60	240	160	1500
Cooling time	60			

2.5. Determination Procedure

2.5.1. HR-ICP-MS

Following ignition, the instrument parameters were initially adjusted at the low-resolution mode to achieve optimal operating conditions (Table 3). Subsequently, the instrument was switched to the medium resolution mode, and the ion optics parameters were fine-tuned to ensure intact peak shape and maximum signal. Mass calibration was then performed, and the standard deviation (SD) value was checked against the previous calibration, with a criterion of less than 150. Once these steps were completed, the instrument was prepared for sample analysis. For detailed information on the HR-ICP-MS analysis procedure, refer to Zhao et al. (2024) [60].

Table 3. Optimized instrumental parameters for HR-ICP-MS.

Items	Values	Items	Values/Status
Plasma RF power	1380 W	Spray chamber temperature	3 ± 0.1 °C
Nebulizer gas pressure	37.8 PSI	Nebulizer	Teflon neb
Auxiliary gas flow	0.8 L/min	Peristaltic pump speed	30 RPM
Coolant gas flow	13 L/min	Dwell time	5 ms
Number of cycles	5 times	Testing time for each run	25 ms

2.5.2. ICP-CCT-MS

When the instrument was stabilized after ignition, the optimization procedure was carried out for the ICP-CCT-MS instrument. The collision gas flow was adjusted from 0 mL/min to 4 mL/min gradually. After a stabilization period of 30 min, the parameters listed in Table 4 were adjusted to maximize the signal of each element in the tuning solution. Following these adjustments, the instrument was ready for sample testing. For a comprehensive description of the ICP-CCT-MS analysis procedure, please refer to Li et al. (2014) [43].

Table 4. Optimized instrumental parameters for ICP-CCT-MS. After Li et al. (2014) [43].

Items	Values	Items	Values/Status
Plasma RF power	1400 W	Nebulizer	Teflon neb
Nebulizer gas flow	1.00 L/min	Collision gas flow	4 mL/min
Auxiliary gas flow	0.8 L/min	Peristaltic pump speed	30 RPM
Coolant gas flow	13.0 L/min	Dwell time	10 ms
Number of main runs	3 times	Testing time for each run	30 ms

3. Results and Discussion

3.1. HR-ICP-MS

3.1.1. Isotope Selection

Selenium has six natural isotopes with relative atomic masses of 74, 76, 77, 78, 80, and 82 [24,51,61,62]. These isotopes can be subject to various interferences during mass spectrometry analysis, which can be categorized into diatomic ion interferences, isobar interferences, and doubly charged ion interferences (Table 5).

Table 5. Interference table of natural isotopes of Selenium.

Isotope	Mass	Abundance (%)	Major Interference
^{74}Se	73.92248	0.87	^{74}Ge; ^{148}Sm^{2+}; ^{148}Nd^{2+}; ^{38}Ar^{36}Ar
^{76}Se	75.91921	9.12	^{76}Ge; ^{152}Sm^{2+}; ^{152}Gd^{2+}; ^{38}Ar$_2$; ^{40}Ar^{36}Ar
^{77}Se	76.91991	7.50	^{154}Sm^{2+}; ^{154}Gd^{2+}; ^{154}BaO^{2+}
^{78}Se	77.91773	23.61	^{156}Gd^{2+}; ^{156}Dy^{2+}; ^{156}CeO^{2+}; ^{40}Ar^{38}Ar
^{80}Se	79.91652	49.96	^{80}Kr; ^{160}Gd^{2+}; ^{160}Dy^{2+}; ^{40}Ar$_2$
^{82}Se	81.91671	8.84	^{82}Kr; ^{164}Dy^{2+}; ^{164}Er^{2+}

Diatomic ion interferences in selenium determination primarily originate from argon. Argon is used as the cooling, auxiliary, and nebulizer gas in the experiment and produces a strong signal in the test system that is challenging to separate even at high resolution. This interference mainly affects the determination of ^{74}Se, ^{76}Se, ^{78}Se, and ^{80}Se.

Isobar interferences primarily impact ^{74}Se, ^{76}Se, ^{80}Se, and ^{82}Se, which may be interfered with by ^{74}Ge, ^{76}Ge, ^{80}Kr, and ^{82}Kr, respectively. Although ^{74}Ge can be separated from ^{74}Se at a low resolution, ^{76}Ge and ^{76}Se have similar atomic masses and can only be separated at a very high resolution (resolution = 34,570 amu). However, achieving such a high resolution poses challenges in maintaining signal strength and instrument stability, thus compromising the accuracy and reliability of results. Common argon separation methods,

such as cryogenic fractionation and pressure friction distillation, have efficient separation capabilities but are not entirely accurate, resulting in residual krypton gas in ultrapure argon gas. This krypton gas interferes with ^{80}Se and ^{82}Se, making it difficult to completely separate or eliminate this interference.

Doubly charged ion interferences in the determination of selenium in coal-bearing strata are mainly from the rare earth elements (such as Sm^{2+}, Nd^{2+}, Gd^{2+}, and Dy^{2+}, etc.). These interferences can typically be effectively separated at medium to high resolution.

Considering the low abundance of ^{74}Se in nature and the difficulties in separating interferences for ^{74}Se, ^{76}Se, ^{78}Se, ^{80}Se, and ^{82}Se, comprehensive consideration led to the selection of ^{77}Se as the isotope for HR-ICP-MS analysis.

3.1.2. Mass Spectral Interference and Correction

The main interference of ^{77}Se comes from the doubly charged ions of rare earth elements and BaO. Table 6 shows that these interferences can be effectively separated within the resolution range of 1867–2525 amu. Therefore, the medium resolution (resolution = 4000 amu) is chosen for determination, allowing for the separation of interfering ions from the elements to be measured without excessively weakening the signal (Figure 1).

Table 6. Interference table of ^{77}Se.

Interferent	Mass	Required Resolution (amu)
^{77}Se	76.91991	
^{154}Sm^{2+}	76.96111	1867
^{154}Gd^{2+}	76.96044	1898
^{154}BaO^{2+}	76.95036	2525
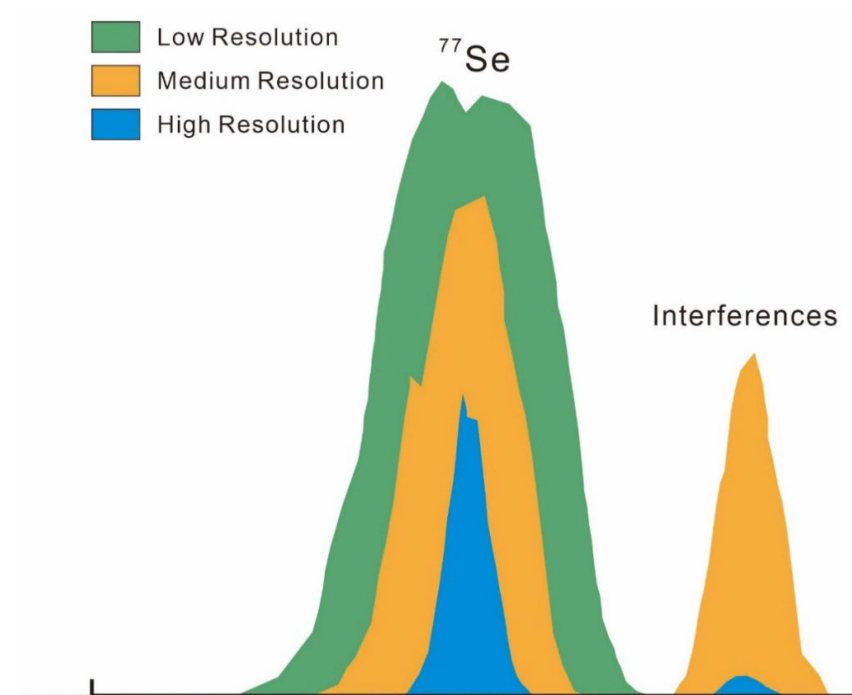
Figure 1. Peak of ^{77}Se at low, medium, and high resolution. At low-resolution mode, the peak of the interferences overlaps with the peak of ^{77}Se. At medium-resolution mode, the peak of the interferences is completely separated from the peak of ^{77}Se. At high-resolution mode, the complete separation is also achieved, but the signal is strongly attenuated.

The results obtained from the actual tests verified the previous theoretical analysis. Taking SRM 2685c as an example, test data for six Se isotopes were obtained in multiple resolution modes, which are recorded in detail in Table 7. Among them, the results for three

isotopes, ^{74}Se, ^{78}Se, and ^{80}Se, are all below the detection limit, while among the remaining three isotopes, ^{77}Se performs particularly well and is in high agreement with the certified value (1.90 μg/g). Based on these results, it can be confirmed that the determination of ^{77}Se by HR-ICP-MS at medium-resolution mode is practical and effective.

Table 7. Observed values (μg/g) of the six Se isotopes in the standard reference sample SRM 2685c of the HR-ICP-MS at different resolutions.

Detection Mode	^{74}Se	^{76}Se	^{77}Se	^{78}Se	^{80}Se	^{82}Se
Low Resolution	bdl	10.59	2.18	bdl	bdl	3.75
Medium Resolution	bdl	9.89	1.94	bdl	bdl	3.02
High Resolution	bdl	9.51	1.86	bdl	bdl	3.01

bdl, below detection limit.

3.2. Results Comparison

The method detection limit (MDL) was determined by calculating three times the standard deviation of the 11 results. The MDL of HR-ICP-MS (0.805 μg/L) was found to be higher than that of ICP-CCT-MS (0.095 μg/L), indicating that the latter method offers better precision (Table 8).

Table 8. Selected elements, calibration curves, and method detection limits (MDLs) of HR-ICP-MS and ICP-CCT-MS.

Instrument	Linearity(μg/L)	Correlation Coefficient	MDL(μg/L)
HR-ICP-MS	0–100	0.999946	0.805
ICP-CCT-MS	0–100	0.999961	0.519

With the relative error (RE) ranging from 0% to 8.28%, HR-ICP-MS provides higher accuracy than ICP-CCT-MS such that the RE was in the range of 1.58%–17.27% (Table 8). The relative standard deviations (RSDs) for HR-ICP-MS and ICP-CCT-MS were observed to range from 5.82% to 8.37% and 4.78% to 9.97%, respectively (Table 9). The internal standard recoveries for HR-ICP-MS and ICP-CCT-MS were found to be in the range of 71.01%–84.56% and 86.56%–119.46%, respectively (Table 9). The lower recoveries obtained from HR-ICP-MS suggest weaker stability when compared to ICP-CCT-MS.

Table 9. Certified (Cer) and observed (Obs) values of Se (μg/g) in the standard reference samples, as well as relative error (RE, %), relative standard deviation (RSD, %), and the internal standard recovery (Rec, %) of the HR-ICP-MS and ICP-CCT-MS.

Sample ID	HR-ICP-MS					ICP-CCT-MS			
	Cer	Obs	RE	RSD	Rec	Obs	RE	RSD	Rec
SRM 1632e	1.53	1.54	0.65	8.37	92.87	1.56	1.96	4.78	119.46
SRM 2685c	1.90	1.94	2.10	7.18	93.44	1.93	1.58	6.67	113.81
SRM 1633c	13.90	13.32	4.17	8.15	71.36	16.30	17.27	5.53	98.16
SRM 2691	17.00	17.78	4.59	6.92	71.01	16.65	2.06	9.97	94.28
GSR-20	29.7	31.58	6.33	5.82	74.04	34.24	15.29	6.80	98.33

The detailed results of 10 consecutive runs of the standard reference material NIST 2685c using HR-ICP-MS and ICP-CCT-MS are listed in Table 10, and the X(bar)—S control charts are plotted accordingly. From Figure 2A,B, no anomalies are found during the consecutive tests for both HR-ICP-MS and ICP-CCT-MS, indicating that the process itself is stable and controlled. However, for both the X(bar) control charts and S control charts, ICP-CCT-MS has a larger range of fluctuations, suggesting that HR-ICP-MS demonstrates greater stability when a large number of samples are measured consecutively.

Table 10. Observed values of Se (µg/g) and standard deviation (SD) for each cycle in the 10 consistent runs of the standard reference material NIST 2685c by HR-ICP-MS and ICP-CCT-MS.

	Run 1	Run 2	Run 3	Run 4	Run 5	Run 6	Run 7	Run 8	Run 9	Run 10	Ave
					HR-ICP-MS						
Cycle 1	2.15	1.86	2.17	1.99	2.00	2.18	2.10	1.75	2.14	2.15	
Cycle 2	1.92	2.13	1.77	1.80	1.67	1.68	1.84	2.04	2.06	1.81	
Cycle 3	1.89	1.89	1.75	2.02	2.03	2.05	1.68	1.88	1.73	1.87	
Cycle 4	1.75	1.88	1.97	2.11	1.97	2.14	2.14	1.96	1.93	1.90	
Cycle 5	1.95	2.04	2.14	1.85	1.97	1.70	1.87	2.00	2.02	1.95	
Ave	1.93	1.96	1.96	1.95	1.93	1.95	1.93	1.93	1.97	1.94	1.94
SD	0.13	0.10	0.18	0.11	0.13	0.22	0.17	0.10	0.14	0.11	0.14
					ICP-CCT-MS						
Cycle 1	2.10	2.02	1.96	2.10	2.12	1.94	1.94	1.76	1.96	1.84	
Cycle 2	1.94	1.90	1.76	1.86	1.84	1.80	2.06	1.98	2.16	1.88	
Cycle 3	1.74	1.88	2.14	1.86	1.94	2.10	1.88	1.76	1.56	2.16	
Ave	1.93	1.93	1.95	1.94	1.97	1.95	1.96	1.83	1.89	1.96	1.93
SD	0.15	0.06	0.16	0.11	0.12	0.12	0.07	0.10	0.25	0.14	0.13
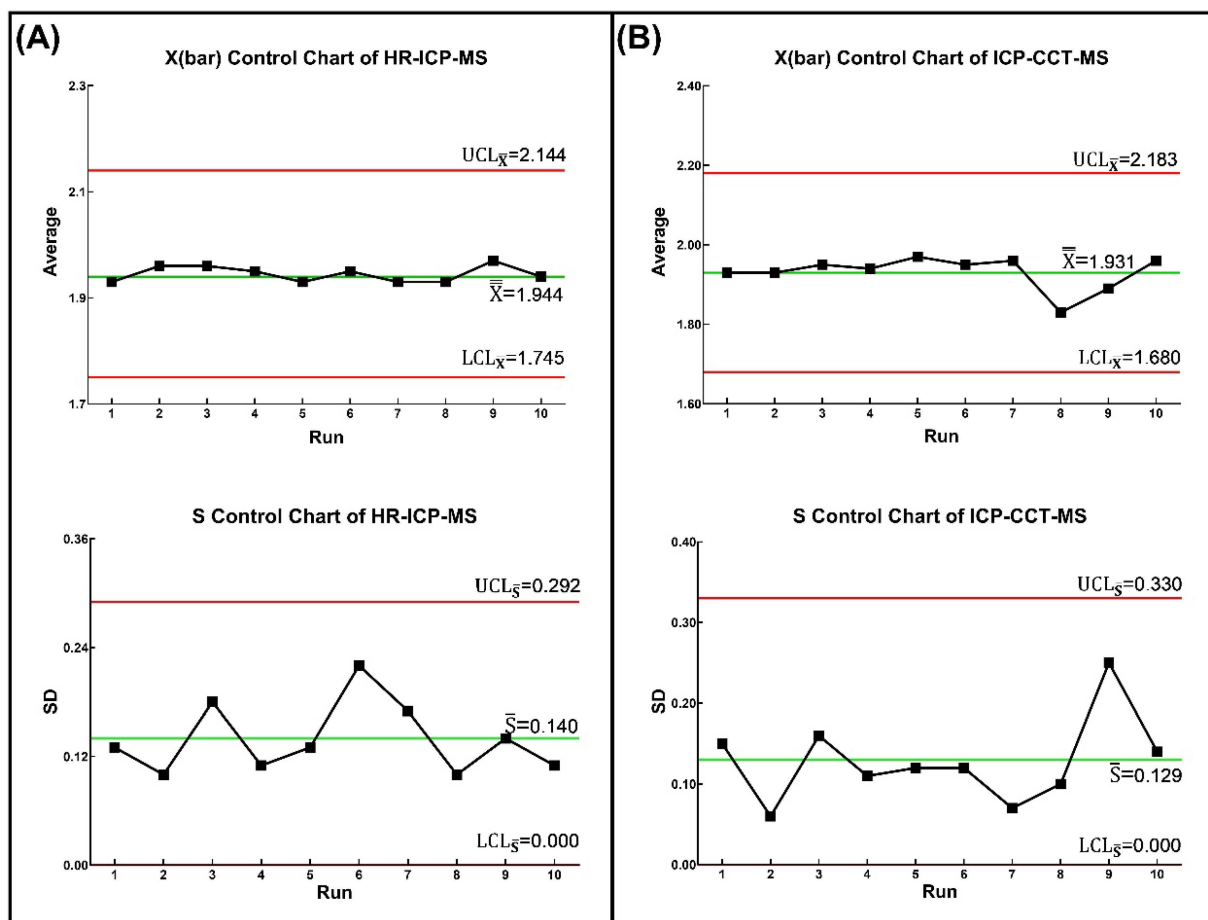
Figure 2. X(bar)—S control charts of NIST 2685c using HR-ICP-MS (**A**) and ICP-CCT-MS (**B**).

The results of the selected coal-bearing strata obtained from HR-ICP-MS and ICP-CCT-MS are generally consistent (Table 11). The internal standard recoveries of ICP-CCT-MS were superior to those of HR-ICP-MS, indicating that ICP-CCT-MS offers better instrumental stability.

Table 11. Observed (Obs) values of Se (μg/g) and the internal standard recovery (Rec, %) of the selected coal-bearing strata samples by HR-ICP-MS and ICP-CCT-MS.

Sample ID	HR-ICP-MS			ICP-CCT-MS		
	Obs	**RSD**	**Rec**	**Obs**	**RSD**	**Rec**
QS-9-1	1.98	4.37	75.34	2.02	17.48	105.25
QS-9-2	3.18	5.28	82.68	3.12	23.56	107.04
QS-9-3	9.97	2.72	80.84	10.28	8.67	108.21
QS-9-4	6.68	3.59	77.75	6.46	8.64	105.76
QS-9-5	5.44	2.16	79.98	5.68	5.15	107.40
QS-9-R	3.73	6.02	70.59	3.63	14.36	113.44
QS-9-6M	6.06	7.65	77.62	6.14	14.56	112.89
QS-9-7M	3.52	3.14	78.44	3.80	8.33	110.45
QS-9-8M	2.96	3.71	71.92	3.05	15.14	110.92
QS-9-F	2.16	4.39	75.64	2.28	17.71	108.78

HR-ICP-MS takes less time (25 ms) than ICP-CCT-MS (30 ms) to test a single sample while testing more cycles with similar results, giving it an advantage in testing a large number of consecutive samples.

4. Conclusions

This study presented an improved method for the determination of Se in coal-bearing strata using HR-ICP-MS. By selecting ^{77}Se as the isotope for analysis and performing the measurement at medium resolution (resolution = 4000 amu), the results obtained from standard reference samples demonstrated close agreement with certified values. This approach proves to be reliable for Se determination in coal-bearing strata, as indicated by the low relative error. HR-ICP-MS exhibits superior stability in continuous determination, albeit with slightly weaker internal standard recovery. In addition, HR-ICP-MS offers the advantages of short test duration, and high accuracy, making it more suitable for the determination of Se in coal-bearing strata.

Author Contributions: Conceptualization, S.Z.; methodology, S.Z., R.J. and Q.H.; formal analysis, S.Z., K.T. and J.F.; data curation, Q.H. and N.S.; writing—original draft preparation, S.Z.; writing—review and editing, S.Z. All authors have read and agreed to the published version of the manuscript.

Data Availability Statement: The data presented in this study are available on request from the corresponding author.

Conflicts of Interest: The authors declare no conflict of interest.

References

1. Arbuzov, S.I.; Chekryzhov, I.Y.; Verkhoturov, A.A.; Spears, D.A.; Melkiy, V.A.; Zarubina, N.V.; Blokhin, M.G. Geochemistry and Rare-Metal Potential of Coals of the Sakhalin Coal Basin, Sakhalin Island, Russia. *Int. J. Coal Geol.* **2023**, *268*, 104197. [CrossRef]
2. Arbuzov, S.I.; Mezhibor, A.M.; Spears, D.A.; Ilenok, S.S.; Shaldybin, M.V.; Belaya, E.V. Nature of Tonsteins in the Azeisk Deposit of the Irkutsk Coal Basin (Siberia, Russia). *Int. J. Coal Geol.* **2016**, *153*, 99–111. [CrossRef]
3. Chatterjee, S.; Mastalerz, M.; Drobniak, A.; Karacan, C.Ö. Machine Learning and Data Augmentation Approach for Identification of Rare Earth Element Potential in Indiana Coals, USA. *Int. J. Coal Geol.* **2022**, *259*, 104054. [CrossRef]
4. Hou, Y.; Dai, S.; Nechaev, V.P.; Finkelman, R.B.; Wang, H.; Zhang, S.; Di, S. Mineral Matter in the Pennsylvanian Coal from the Yangquan Mining District, Northeastern Qinshui Basin, China: Enrichment of Critical Elements and a Se-Mo-Pb-Hg Assemblage. *Int. J. Coal Geol.* **2023**, *266*, 104178. [CrossRef]
5. Karayigit, A.I.; Yerin, Ü.O.; Oskay, R.G.; Bulut, Y.; Córdoba, P. Enrichment and Distribution of Elements in the Middle Miocene Coal Seams in the Orhaneli Coalfield (NW Turkey). *Int. J. Coal Geol.* **2021**, *247*, 103854. [CrossRef]

6. Liu, J.; Dai, S.; Song, H.; Nechaev, V.P.; French, D.; Spiro, B.F.; Graham, I.T.; Hower, J.C.; Shao, L.; Zhao, J. Geological Factors Controlling Variations in the Mineralogical and Elemental Compositions of Late Permian Coals from the Zhijin-Nayong Coalfield, Western Guizhou, China. *Int. J. Coal Geol.* **2021**, *247*, 103855. [CrossRef]

7. Wang, N.; French, D.; Dai, S.; Graham, I.T.; Zhao, L.; Song, X.; Zheng, J.; Gao, Y.; Wang, Y. Origin of Chamosite and Berthierine: Implications for Volcanic-Ash-Derived Nb-Zr-REY-Ga Mineralization in the Lopingian Sequences from Eastern Yunnan, SW China. *J. Asian Earth Sci.* **2023**, *253*, 105703. [CrossRef]

8. Hamilton, S.J. Review of Selenium Toxicity in the Aquatic Food Chain. *Sci. Total Environ.* **2004**, *326*, 1–31. [CrossRef]

9. Tinggi, U. Essentiality and Toxicity of Selenium and Its Status in Australia: A Review. *Toxicol. Lett.* **2003**, *137*, 103–110. [CrossRef]

10. Dinh, Q.T.; Cui, Z.; Huang, J.; Tran, T.A.; Wang, D.; Yang, W.; Zhou, F.; Wang, M.; Yu, D.; Liang, D. Selenium Distribution in the Chinese Environment and Its Relationship with Human Health: A Review. *Environ. Int.* **2018**, *112*, 294–309. [CrossRef]

11. Wang, L.; Ju, Y.; Liu, G.; Chou, C.-L.; Zheng, L.; Qi, C. Selenium in Chinese Coals: Distribution, Occurrence, and Health Impact. *Environ. Earth Sci.* **2009**, *60*, 1641–1651. [CrossRef]

12. Dai, S.; Ren, D.; Chou, C.-L.; Finkelman, R.B.; Seredin, V.V.; Zhou, Y. Geochemistry of Trace Elements in Chinese Coals: A Review of Abundances, Genetic Types, Impacts on Human Health, and Industrial Utilization. *Int. J. Coal Geol.* **2012**, *94*, 3–21. [CrossRef]

13. Sun, H.-J.; Rathinasabapathi, B.; Wu, B.; Luo, J.; Pu, L.-P.; Ma, L.Q. Arsenic and Selenium Toxicity and Their Interactive Effects in Humans. *Environ. Int.* **2014**, *69*, 148–158. [CrossRef] [PubMed]

14. Taylor, J.B.; Reynolds, L.P.; Redmer, D.A.; Caton, J.S. Maternal and Fetal Tissue Selenium Loads in Nulliparous Ewes Fed Supranutritional and Excessive Selenium during Mid- to Late Pregnancy1,2. *J. Anim. Sci.* **2009**, *87*, 1828–1834. [CrossRef] [PubMed]

15. Chen, X.; Yang, G.; Chen, J.; Chen, X.; Wen, Z.; Ge, K. Studies on the Relations of Selenium and Keshan Disease. *Biol. Trace Elem. Res.* **1980**, *2*, 91–107. [CrossRef]

16. Klein, E.A. Selenium: Epidemiology and Basic Science. *J. Urol.* **2004**, *171*, S50–S53. [CrossRef]

17. Lemly, A.D. Selenium Poisoning of Fish by Coal Ash Wastewater in Herrington Lake, Kentucky. *Ecotoxicol. Environ. Saf.* **2018**, *150*, 49–53. [CrossRef]

18. Chua, E.M.; Flint, N.; Wilson, S.P.; Vink, S. Potential for Biomonitoring Metals and Metalloids Using Fish Condition and Tissue Analysis in an Agricultural and Coal Mining Region. *Chemosphere* **2018**, *202*, 598–608. [CrossRef] [PubMed]

19. Ma, S.; Xu, F.; Qiu, D.; Fan, S.; Wang, R.; Li, Y.; Chen, X. The Occurrence, Transformation and Control of Selenium in Coal-Fired Power Plants: Status Quo and Development. *J. Air Waste Manag. Assoc.* **2022**, *72*, 131–146. [CrossRef]

20. Niu, C.; Luo, K. Relationship of Selenium, Arsenic and Sulfur in Soil and Plants in Enshi County, China. *J. Food Agric. Environ.* **2011**, *9*, 646–651.

21. Shah, P.; Strezov, V.; Stevanov, C.; Nelson, P.F. Speciation of Arsenic and Selenium in Coal Combustion Products. *Energy Fuels* **2006**, *21*, 506–512. [CrossRef]

22. Tang, Q.; Liu, G.; Yan, Z.; Sun, R. Distribution and Fate of Environmentally Sensitive Elements (Arsenic, Mercury, Stibium and Selenium) in Coal-Fired Power Plants at Huainan, Anhui, China. *Fuel* **2012**, *95*, 334–339. [CrossRef]

23. Xie, J.; Niu, X.-D.; He, K.-Q.; Shi, M.-D.; Yu, S.-J.; Yuan, C.-G.; Liu, J.-F. Arsenic and Selenium Distribution and Speciation in Coal and Coal Combustion By-Products from Coal-Fired Power Plants. *Fuel* **2021**, *292*, 120228. [CrossRef]

24. Zhang, Q.; Wu, B.; Wu, J.; Qi, Y.; Chu, W.; Qiao, L.; Zhang, B.; Shen, P.; Tang, T. Study on Arsenic, Selenium, and Lead Produced in Coal Combustion: Bibliometric Method. *Environ. Sci. Pollut. Res.* **2021**, *28*, 32190–32199. [CrossRef] [PubMed]

25. Finkelman, R.B.; Orem, W.; Castranova, V.; Tatu, C.A.; Belkin, H.E.; Zheng, B.; Lerch, H.E.; Maharaj, S.V.; Bates, A.L. Health Impacts of Coal and Coal Use: Possible Solutions. *Int. J. Coal Geol.* **2002**, *50*, 425–443. [CrossRef]

26. Song, G.; Xu, W.; Liu, K.; Song, Q. Transformation of Selenium during Coal Thermal Conversion: Effects of Atmosphere and Inorganic Content. *Fuel Process. Technol.* **2020**, *205*, 106446. [CrossRef]

27. Díaz-Somoano, M.; Antonia López-Antón, M.; Rosa Martínez-Tarazona, M. Determination of Selenium by ICP-MS and HG-ICP-MS in Coal, Fly Ashes and Sorbents Used for Flue Gas Cleaning. *Fuel* **2004**, *83*, 231–235. [CrossRef]

28. Huang, Y.; Gong, H.; Hu, H.; Fu, B.; Yuan, B.; Li, S.; Luo, G.; Yao, H. Migration and Emission Behavior of Arsenic and Selenium in a Circulating Fluidized Bed Power Plant Burning Arsenic/Selenium-Enriched Coal. *Chemosphere* **2021**, *263*, 127920. [CrossRef] [PubMed]

29. Swanson, S.M.; Engle, M.A.; Ruppert, L.F.; Affolter, R.H.; Jones, K.B. Partitioning of Selected Trace Elements in Coal Combustion Products from Two Coal-Burning Power Plants in the United States. *Int. J. Coal Geol.* **2013**, *113*, 116–126. [CrossRef]

30. Itskos, G.; Itskos, S.; Moutsatsou, A.; Vasilatos, C.; Koukouzas, N.; Kakaras, E. The Outcomes of the 2-Decade Monthly Monitoring of Fly Ash-Composition in a Lignite-Fired Power Station. *Waste Biomass Valorization* **2010**, *1*, 431–437. [CrossRef]

31. Itskos, G.; Koukouzas, N.; Vasilatos, C.; Megremi, I.; Moutsatsou, A. Comparative Uptake Study of Toxic Elements from Aqueous Media by the Different Particle-Size-Fractions of Fly Ash. *J. Hazard. Mater.* **2010**, *183*, 787–792. [CrossRef] [PubMed]

32. Helble, J.J. Trace Element Behavior during Coal Combustion: Results of a Laboratory Study. *Fuel Process. Technol.* **1994**, *39*, 159–172. [CrossRef]

33. Germani, M.S.; Zoller, W.H. Vapor-phase Concentrations of Arsenic, Selenium, Bromine, Iodine, and Mercury in the Stack of a Coal-fired Power-plant. *Environ. Sci. Technol.* **1988**, *22*, 1079–1085. [CrossRef] [PubMed]

34. *ASTM D 4606-03*; Annual Book of ASTM Standards. Standard Test Method for Determination of Arsenic and Selenium in Coal by the Hydride Generation/Atomic Absorption Method. Gaseous Fuels: Coal and Coke. ASTM International: West Conshohocken, PA, USA, 2007; Volume 05.06.

35. Coufalík, P.; Zvěřina, O.; Sádovská, K.; Komárek, J. UV-Photochemical Vapor Generation Coupled to Hydride Generation AAS in the Study of Dietary Intake of Se, Hg, Cd, and Pb from Fish. *J. Food Compos. Anal.* **2023**, *124*, 105668. [CrossRef]

36. De Oliveira, R.M.; Antunes, A.C.; Vieira, M.A.; Medina, A.L.; Ribeiro, A.S. Evaluation of Sample Preparation Methods for the Determination of As, Cd, Pb, and Se in Rice Samples by GF AAS. *Microchem. J.* **2016**, *124*, 402–409. [CrossRef]

37. Shaltout, A.A.; Bouslimi, J.; Besbes, H. The Challenges of Se Quantification in Bean Samples Using Line and Continuum Sources Atomic Absorption Spectrometry. *Food Chem.* **2020**, *328*, 127124. [CrossRef] [PubMed]

38. Sánchez-Rodas, D.; Corns, W.T.; Chen, B.; Stockwell, P.B. Atomic Fluorescence Spectrometry: A Suitable Detection Technique in Speciation Studies for Arsenic, Selenium, Antimony and Mercury. *J. Anal. At. Spectrom.* **2010**, *25*, 933. [CrossRef]

39. Xie, X.; Feng, C.; Ye, M.; Wang, C. Speciation Determination of Selenium in Seafood by High-Performance Ion-Exchange Chromatography-Hydride Generation-Atomic Fluorescence Spectrometry. *Food Anal. Methods* **2014**, *8*, 1739–1745. [CrossRef]

40. Iwashita, A.; Nakajima, T.; Takanashi, H.; Ohki, A.; Fujita, Y.; Yamashita, T. Determination of Trace Elements in Coal and Coal Fly Ash by Joint-Use of ICP-AES and Atomic Absorption Spectrometry. *Talanta* **2007**, *71*, 251–257. [CrossRef]

41. Yan, Q.; Yang, L.; Wang, Q.; Ma, X. Determination of Major and Trace Elements in Six Herbal Drugs for Relieving Heat and Toxicity by ICP-AES with Microwave Digestion. *J. Saudi Chem. Soc.* **2012**, *16*, 287–290.

42. Sihlahla, M.; Mpupa, A.; Sojka, M.; Saeid, A.; Nomngongo, P.N. Determination of Selenium in Cereal and Biofortified Samples by ICP-OES Using an Alcohol-Based Deep Eutectic Solvent in Digestion Procedure. *Adv. Sample Prep.* **2023**, *8*, 100092. [CrossRef]

43. Li, X.; Dai, S.; Zhang, W.; Li, T.; Zheng, X.; Chen, W. Determination of As and Se in Coal and Coal Combustion Products Using Closed Vessel Microwave Digestion and Collision/Reaction Cell Technology (CCT) of Inductively Coupled Plasma Mass Spectrometry (ICP-MS). *Int. J. Coal Geol.* **2014**, *124*, 1–4. [CrossRef]

44. Kapilna, E.; Shah, M.; Caruso, J.; Fodor, P. Selenium Speciation Studies in Se-Enriched Chives (Allium Schoenoprasum) by HPLC-ICP–MS. *Food Chem.* **2007**, *101*, 1398–1406. [CrossRef]

45. Montesbayon, M.; Molet, M.; Gonzalez, E.; Sanzmedel, A. Evaluation of Different Sample Extraction Strategies for Selenium Determination in Selenium-Enriched Plants (*Allium sativum* and *Brassica juncea*) and Se Speciation by HPLC-ICP-MS. *Talanta* **2006**, *68*, 1287–1293. [CrossRef] [PubMed]

46. Tie, M.; Li, B.; Sun, T.; Guan, W.; Liang, Y.; Li, H. HPLC-ICP-MS Speciation of Selenium in Se-Cultivated Flammulina Velutipes. *Arab. J. Chem.* **2020**, *13*, 416–422. [CrossRef]

47. Dufailly, V.; Noël, L.; Guérin, T. Determination of Chromium, Iron and Selenium in Foodstuffs of Animal Origin by Collision Cell Technology, Inductively Coupled Plasma Mass Spectrometry (ICP-MS), after Closed Vessel Microwave Digestion. *Anal. Chim. Acta* **2006**, *565*, 214–221. [CrossRef]

48. Dufailly, V.; Noël, L.; Guérin, T. Optimisation and Critical Evaluation of a Collision Cell Technology ICP-MS System for the Determination of Arsenic in Foodstuffs of Animal Origin. *Anal. Chim. Acta* **2008**, *611*, 134–142. [CrossRef] [PubMed]

49. Rowan, J.T.; Houk, R.S. Attenuation of Polyatomic Ion Interferences in Inductively Coupled Plasma Mass Spectrometry by Gas-Phase Collisions. *Appl. Spectrosc.* **1989**, *43*, 976–980. [CrossRef]

50. Tanner, S.D.; Baranov, V.I.; Bandura, D.R. Reaction Cells and Collision Cells for ICP-MS: A Tutorial Review. *Spectrochim. Acta Part B At. Spectrosc.* **2002**, *57*, 1361–1452. [CrossRef]

51. Henn, A.S.; Rondan, F.S.; Mesko, M.F.; Mello, P.A.; Perez, M.; Armstrong, J.; Bullock, L.A.; Parnell, J.; Feldmann, J.; Flores, E.M.M. Determination of Se at Low Concentration in Coal by Collision/Reaction Cell Technology Inductively Coupled Plasma Mass Spectrometry. *Spectrochim. Acta Part B At. Spectrosc.* **2018**, *143*, 48–54. [CrossRef]

52. Sánchez-Rodas, D.; Mellano, F.; Martínez, F.; Palencia, P.; Giráldez, I.; Morales, E. Speciation Analysis of Se-Enriched Strawberries (Fragaria Ananassa Duch) Cultivated on Hydroponics by HPLC-TR-HG-AFS. *Microchem. J.* **2016**, *127*, 120–124. [CrossRef]

53. Wang, M.; Zhong, Y.; Qin, J.; Zhang, Z.; Li, S.; Yang, B. Determination of Total Selenium in Food Samples by D-CPE and HG-AFS. *Food Chem.* **2017**, *227*, 329–334. [CrossRef] [PubMed]

54. García, J.B.; Krachler, M.; Chen, B.; Shotyk, W. Improved Determination of Selenium in Plant and Peat Samples Using Hydride Generation-Atomic Fluorescence Spectrometry (HG-AFS). *Anal. Chim. Acta* **2005**, *534*, 255–261. [CrossRef]

55. Yang, J.; Chen, Y.; Shi, K.; Hu, K.; Li, R.; Gao, X.; Wang, Q.; Zhang, W.; Zhou, Y.; Wang, Y.; et al. Stability of Selenium and Its Speciation Analysis in Water Using Automatic System Separation and HR-ICP-MS Measurement. *Chin. Chem. Lett.* **2022**, *33*, 3444–3450. [CrossRef]

56. Balaram, V.; Rahaman, W.; Roy, P. Recent Advances in MC-ICP-MS Applications in Earth and Environmental Sciences: Challenges and Solutions. *Geosystems Geoenviron.* **2022**, *1*, 100019. [CrossRef]

57. Hanousek, O.; Brunner, M.; Pröfrock, D.; Irrgeher, J.; Prohaska, T. The Performance of Single and Multi-Collector ICP-MS Instruments for Fast and Reliable ^{34}S/^{32}S Isotope Ratio Measurements. *Anal. Methods* **2016**, *8*, 7661–7672. [CrossRef]

58. Satyanarayanan, M.; Balaram, V.; Sawant, S.S.; Subramanyam, K.S.V.; Vamsi Krishna, G.; Dasaram, B.; Manikyamba, C. Rapid Determination of REEs, PGEs, and Other Trace Elements in Geological and Environmental Materials by High Resolution Inductively Coupled Plasma Mass Spectrometry. *At. Spectrosc.* **2018**, *39*, 1–15. [CrossRef]

59. Evans, E.H.; Giglio, J.J. Interferences in Inductively Coupled Plasma Mass Spectrometry. A Review. *J. Anal. At. Spectrom.* **1993**, *8*, 18. [CrossRef]

60. Zhao, S.; Liu, J.; Jia, R.; Feng, J.; Teng, K.; Han, Q.; Shang, N. Precise Determination of Eu Concentration in Coal and Sedimentary Rock Samples Using High-Resolution Inductively Coupled Plasma Mass Spectrometry (HR-ICP-MS). *Minerals* **2023**, *1*, 8. [CrossRef]
61. Yudovich, Y.E.; Ketris, M.P. Selenium in Coal: A Review. *Int. J. Coal Geol.* **2006**, *67*, 112–126. [CrossRef]
62. Gross, J.L.; Claes, J.; Kathawa, J.; Thoennessen, M. Discovery of Zinc, Selenium, Bromine, and Neodymium Isotopes. *At. Data Nucl. Data Tables* **2012**, *98*, 75–94. [CrossRef]